Thermoanalytical studies on the thermal and catalytic decomposition of aqueous hydroxylammonium nitrate solution

Alan A. Esparza, Robert E. Ferguson, Ahsan Choudhuri, Norman D. Love, Evgeny Shafirovich*

Department of Mechanical Engineering, The University of Texas at El Paso, El Paso, TX 79968, USA

ARTICLE INFO

ABSTRACT

Green monopropellants based on hydroxylammonium nitrate (HAN) are a promising alternative to hydrazine in space propulsion systems. In the present paper, thermal and catalytic decomposition of aqueous HAN solution was studied using thermogravimetric analysis (TGA), differential scanning calorimetry (DSC), and mass spectrometry. The tests were conducted at heating rates of 1, 2.5, 5, and 10 K/min. The values of the apparent activation energy obtained for thermal decomposition using TGA and DSC are 62.2 ± 3.7 kJ/mol and 57.5 ± 3.5 kJ/mol, respectively, and they are in agreement with the literature data for solid HAN and solutions with high concentrations of HAN. The obtained values of the pre-exponential factor, 2.24×10^4 s^{-1} for TGA and 3.55×10^3 s^{-1} for DSC, are lower by six to seven orders of magnitude than those reported in the literature for aqueous HAN solutions, apparently because of full vaporization of water from the HAN solution at the beginning of the TGA and DSC tests. The use of an iridium/rhodium foam catalyst decreased the temperature of full decomposition by over 60 °C. The value of the apparent activation energy obtained for the catalytic decomposition using TGA is 63.9 ± 2.5 kJ/mol, while the obtained value of the pre-exponential factor is 3.31×10^5 s^{-1}.

© 2018 The Combustion Institute. Published by Elsevier Inc. All rights reserved.
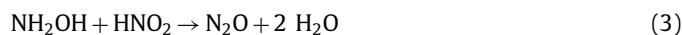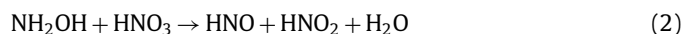
1. Introduction

The replacement of hydrazine by "green" monopropellants based on hydroxylammonium nitrate (HAN, NH_3OHNO_3) is of great interest today because of their relatively low toxicity, high density, high specific impulse, and low freezing point [1–3]. However, some features of their decomposition process hinder their implementation. For example, HAN-based monopropellants generate higher temperatures than hydrazine, thus creating more severe conditions in the thruster than in the case of hydrazine. Also, in contrast with hydrazine, HAN does not decompose on an iridium catalyst at room temperature. The required preheating (300–400 °C) leads to additional energy consumption and a more complicated design of a catalyst bed. To develop an effective propulsion system that uses a HAN-based monopropellant, it is necessary to know the reaction mechanism and kinetic parameters of HAN's catalytic decomposition.

Thermal decomposition of HAN and its aqueous solutions has been studied for many years for liquid gun and rocket propellant applications. It has been shown that the products of HAN decomposition include H_2O, NO, N_2O, NO_2, N_2, and HNO_3 [4–9]. Cronin

and Brill [4,5] have suggested that an early step in the decomposition of HAN is proton transfer from NH_3OH^+ to NO_3^-, which produces hydroxylamine (NH_2OH) and nitric acid (HNO_3):

$$NH_3OHNO_3 \rightarrow NH_2OH + HNO_3 \tag{1}$$

Oxley and Brower [6] have proposed the reaction mechanism that includes this step and subsequent oxidation of hydroxylamine by HNO_3 and formed HNO_2 and HNO:

$$NH_2OH + HNO_3 \rightarrow HNO + HNO_2 + H_2O \tag{2}$$

$$NH_2OH + HNO_2 \rightarrow N_2O + 2\ H_2O \tag{3}$$

$$NH_2OH + HNO \rightarrow N_2 + 2\ H_2O \tag{4}$$

$$HNO + HNO_3 \rightarrow 2\ HNO_2 \tag{5}$$

This mechanism, however, did not involve the formation of NO, observed in the experiments [5–9]. Also, NO_2 formation was not included though the authors observed its formation in their FTIR tests and discussed the reaction between HNO_2 and HNO_3 that produces NO_2:

$$HNO_2 + HNO_3 \rightarrow 2\ NO_2 + H_2O \tag{6}$$

Lee and Litzinger [9] have added the reaction of NO_2 formation (Eq. (6)) and two additional steps:

$$2\ HNO \rightarrow N_2O + H_2O \tag{7}$$

$$3\ HNO_2 \rightarrow 2\ NO + HNO_3 + H_2O \tag{8}$$
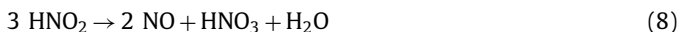
The resulting mechanism (Eqs. (1)–(8)) explains the formation of all species detected in the experiments.

Several research teams have reported kinetic parameters of thermal decomposition of HAN. Rafeev and Rubtsov [10] obtained an activation energy (E_a) of 64 kJ/mol for thermal decomposition of solid HAN. Shaw and Williams [11] developed a model for deflagration of HAN-H_2O mixtures. Using this model and experimental data [12] on the deflagration velocity in these mixtures (5.2–9.1 M solutions), they have obtained the activation energy in the range from 61 to 71 kJ/mol and a pre-exponential factor (A) in the range of 3.05×10^{10} to 4.94×10^{10} s^{-1}. They have also noted that the obtained values of the activation energy are close to the estimated endothermicity, about 70 kJ/mol, of the proton transfer reaction (Eq. (1)), which apparently controls the rate of HAN decomposition. Lee and Litzinger [9] deduced $E_a = 63.2 \pm 2.1$ kJ/mol and $A = 1.7 \times 10^{10} \pm 9.3 \times 10^2$ s^{-1} for the proton transfer reaction (Eq. (1)). Schoppelrei and Brill [13,14] noticed that the apparent activation energy increases with decreasing of the concentration of HAN in its aqueous solution; the higher concentrations of HAN yield E_a in the 60–70 kJ/mol range though E_a values above 100 kJ/mol are possible for lower concentrations. They suggested that at lower concentrations the oxidation of hydroxylamine by HNO_3 (Eq. (2)) controls the overall rate, while at higher concentrations the autocatalysis, possibly by the formed HNO_2, accelerates the rate of reaction and release of heat, giving a lower apparent activation energy [13]. More recently, Liu et al. [15] studied autocatalytic decomposition of HAN aqueous solution (24 wt% HAN) in an adiabatic calorimeter and deduced $E_a = 82.0 \pm 0.4$ kJ/mol and $A = 7 \times 10^5$ s^{-1} as well as other parameters of the observed autocatalytic reaction.

Since the use of HAN-based monopropellants involves a catalyst, it is important to understand the effect of catalyst on the decomposition of HAN. Several research teams have investigated catalytic decomposition of HAN and HAN-based monopropellants. A brief review of early tests of different catalysts for HAN decomposition is available [16]. In recent years, iridium-based catalysts have been in the focus of research on catalytic decomposition of HAN and HAN-based monopropellants [2,3,17–21]. It has been shown that the Ir-based catalyst lowers the onset temperature of HAN decomposition [21].

This brief review implies that more research is needed to obtain reliable information on the thermal and catalytic decomposition of HAN. There are significant discrepancies in the kinetic parameters of thermal decomposition reported by different research teams. For the catalytic decomposition, the reaction mechanism is unclear and the kinetic parameters remain unknown. The objective of the present work is to determine effective kinetic parameters for both non-catalytic (thermal) and catalytic decomposition of aqueous HAN solution using thermoanalytical methods as well as to obtain information on the evolved gas products using mass spectrometry.

2. Experimental

Decomposition of aqueous HAN solution (24 wt% HAN, 99.999% pure, Sigma-Aldrich) was studied using a thermogravimetric analyzer (Netzsch TG 209 F1 Iris), a differential scanning calorimeter (Netzsch DSC 404 F1 Pegasus), and a quadrupole mass spectrometer (Netzch QMS 403D Aëolos).

In TGA tests, 10 µL of solution were placed using a pipette (Oxford Benchmate 10–100 µL) in alumina crucibles and heated in a 70 mL/min argon flow at different heating rates over the range from 1 to 10 K/min. The initial tests were performed with a 10-min isothermal step to purge air from the furnace prior to heating, while the subsequent tests involved three vacuum cycles instead of the 10-min isothermal step. DSC trials were conducted at heating rates from 1 to 50 K/min in a 20 mL/min argon flow using three vacuum cycles. For catalytic decomposition, iridium/rhodium foam pellets (diameter: 5 mm, height: 2 mm, 100 pores per inch, Ultramet) were placed in the crucibles. For accurate determination of the onset, offset, and area of the DSC peaks, additional temperature and sensitivity calibrations at different heating rates were performed before testing. The TGA microbalance was also calibrated. Further, correction runs for all crucibles and heating rates were carried out prior to TGA and DSC tests. The mass spectrometer was coupled with the TGA instrument via a transfer line heated to 150 °C. This allowed for detection of gases evolved at different stages of the decomposition process during TGA testing.

The data obtained in the thermoanalytical tests at different heating rates were analyzed using Netzsch Thermokinetics software and the Ozawa–Flynn–Wall method [22,23] to determine the apparent activation energy and pre-exponential factor.

3. Results and discussion

3.1. Thermal decomposition of aqueous HAN solution

Initially, thermogravimetric analysis of aqueous HAN solution was conducted with a 10-min isothermal step before heating. Figure 1 shows the TG curve obtained at a heating rate of 10 K/min. The initial drop in mass is explained by evaporation of water, while the second stage of mass loss is associated with HAN decomposition.

Although the initial mass loss correlates with the water content in the solution, it cannot be excluded that some bonded water still remains at temperatures above the water boiling point and may influence the decomposition kinetics. Therefore, for a more accurate determination of HAN decomposition kinetic parameters, all subsequent TGA tests were carried out with three vacuum cycles before heating. Comparison of the measured mass loss with the concentration of water in the initial solution shows that after three vacuum cycles all water was evaporated. Although some traces of water could remain, they probably would be vaporized with approaching the boiling point of water during the relatively slow heating process, so the potential effect of water on the decomposition of HAN would be negligible. Figure 2 shows TG curves obtained in such a procedure at heating rates of 1, 2.5, 5, and 10 K/min. It is seen that, in contrast with Fig. 1, the TG curves are smooth and there is only one stage of mass loss, caused by HAN decomposition. It is also seen that an increase in the heating rate increases the decomposition temperature. At 1 K/min HAN was fully decomposed at about 160 °C, while at 10 K/min the decomposition was complete at about 220 °C.

The apparent activation energy and pre-exponential factor were determined using the Ozawa–Flynn–Wall method, which assumes the first-order kinetics. Figure S1 in the Supplementary Material shows the Ozawa–Flynn–Wall analysis at different conversion rates, while Fig. S2 presents the values of the activation energy and pre-exponential factor as a function of conversion, calculated based on the data shown in Fig. S1. It is seen that the kinetic parameters significantly increase with increasing the conversion from 2% to 15%, but change only slightly with further increasing the conversion. Only after loss of 60% mass, the activation energy starts to decrease significantly. The approximate constancy of the kinetic parameters over a wide range of the conversion degrees validates